Critical Chloride Concentration of Rebar Corrosion in Fly Ash Concrete

Congtao Sun[1], Shiqun Liu[2,], Jiangang Niu[3], Weichen Xu[1]*

[1] Institute of Oceanology Chinese Academy of Science, Qingdao 266071, P.R. China
[2] Architectural Design and Research Institute of Qingdao University, Qingdao 266033, P.R. China
[3] Inner Mongolia University of Science and Technology, Baotou 014010, P.R. China
[*]E-mail: liushiqunqingdao@163.com

Electrochemical impedance spectrum has been used in this work to study the critical chloride concentration for the rebar corrosion in fly ash concrete. The analysis and criteria for the critical corrosion point of rebar have been interpreted, and the surface morphology of the corroded rebar has been studied using SEM. The influences of the wet-dry cycling period and the fly ash content on the impedance spectra and the critical chloride concentration have been discussed respectively. It shows that the critical corrosion point can be precisely manifested by impedance spectra; the resistance of the concrete layer increases with increasing period of wet-dry cycling and increasing content of fly ash, which can be observed as translation of the spectra to the right on the complex plane; the critical chloride concentration tends to increase with increasing period of wet-dry cycling; the critical chloride concentration for rebar corrosion can be increased by a small dosage of fly ash in the concrete.

1. INTRODUCTION

Critical chloride concentration is significant for the prediction of durability of concrete structures, and is also essential for the design, test and maintenance of structures. Critical chloride concentration can be defined in two ways. One definition is from the aspect of scientific research: the highest chloride concentration in the surrounding electrolyte in the pores of concrete, which would not induce depassivation. The other definition is from the aspect of practical engineering: the chloride concentration in the surrounding electrolyte in the pores of concrete, which just induces visible or acceptable corrosion. However, due to the difficulty of quantifying the visible or acceptable corrosion

in the latter definition, the results differ among different researchers. Therefore, the former definition of the critical chloride concentration has been used more widely and frequently[1,2].

There has been a lot of work about the study on critical chloride concentration[2-8], however, the experimental data are scattered, which may be ascribed to the various measurement methods on the corrosion of rebar[6]. Furthermore, different criteria are applied for different methods, which directly affect the values of the critical chloride concentration. In addition, the method to obtain the sample from the surrounding rebar environment at the onset of corrosion is also very important. Therefore, the criteria for the onset of rebar corrosion and the proper method to obtain specimens from the surrounding rebar environment can both help minimize the scattering of the critical chloride concentration value. Meanwhile, they also make it possible for the practical application of the experimental data.

Ac impedance method has been used in this work to monitor and manifest the onset of the rebar corrosion in the concrete. The influence of the wet-dry cycling period and the fly ash content in the concrete on the impedance spectra and critical chloride concentration have been analyzed and discussed. This work should provide reference on manifesting the onset of rebar corrosion, the design for durability and service life prediction of structures.

2. EXPERIMENTAL METHOD

2.1 Raw materials and mix proportion of concrete

P.O42.5 ordinary Portland cement; the local river sand, fineness modulus of 2.9, medium sand; basalt, size 5~20 mm; original state of fly ash level Ⅱ; high efficiency water reducing agent, water reducing rate is 25% ~ 30%; tap water. Concrete mix proportion as shown in Table 1.

Table 1. Mix proportion of concrete

Specimen	Material Consumption （kg/m³)					Water reducer
	Cement	Fly ash	Water	Sand	Crushed stone	
A	400	0	160	662.4	1177.6	1.0%
B	360	40	160	662.4	1177.6	1.0%
C	320	80	160	662.4	1177.6	1.0%

2.2 Preparation of specimens

The HRB335 grade Φ10 rebar was grounded, and the rust and corrosion products on the surface were removed. One side of the rebar was connected with a 500 mm long electric cable and degreased with acetone. Then Φ16 heat-shrinkable tube and hot melt glue were used to seal the end of the rebar, so that the exposed part was 20 mm long as a rebar electrode, which was fixed within a

100×100×300 mm steel mould using two pieces of plastic end plate, and the concrete protective layer was 15 mm thick. After molding for 24 h, specimens were demoulded and kept curing for 56 days. Both ends and two sides of the specimen were sealed with epoxy resin, with only the top and bottom sides exposed in chloride electrolyte.

2.3 Wet-dry cycling

For the wet process, the concrete specimen was immersed in 3.5% NaCl. For the dry process, the specimen was dried in an oven in 50°C. The wet-dry cycling was carried out by controlling the time of immersing and drying. The details of the process are shown in Table 2.

Table 2. Wet-dry cycling test system

Specimen	Serial Number	Cycle Time(h)	Dry-wet Cycling System
A	A	72	3:1(54:18)
B	B1	72	3:1(54:18)
	B2	96	3:1(72:24)
	B3	144	3:1(108:36)
C	C	72	3:1(54:18)

2.4 Monitoring the onset of rebar corrosion

Electrochemical impedance spectrum (EIS) was applied for the monitoring of the rebar corrosion at room temperature. The electrochemical workstation was a PARSTAT®-2273 Advanced Electrochemical System, and a three electrode system was used. At open circuit potential, the amplitude was 10mv, and the frequency was between 0.01 Hz and 105 Hz, with 9 points recorded in each decade. The schematic diagram is shown in Fig.1.
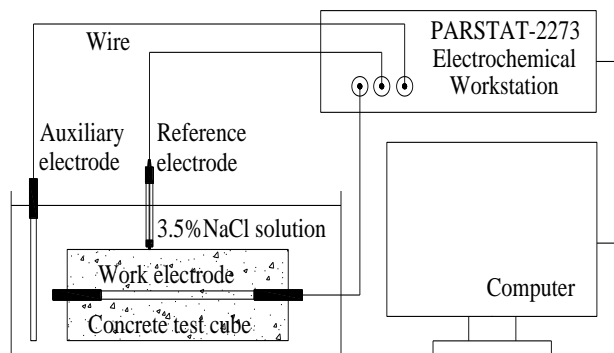
Figure 1. Schematic diagram of the testing of AC impedance

The procedure is as follows. The specimen was immersed in 3.5% NaCl, and OCP was measured to test the stability of the system. If the change of the OCP was less than ±2 mV within 5 min, the system can be regarded as in a steady-state, indicating that EIS measurement can be carried out. The wet-dry cycling continued until corrosion of rebar took place. At the onset of corrosion, linear polarization (LPR) and Tafel polarization were applied which may confirm the onset of corrosion. The LPR was carried out between -20 mV and +20 mV with respect to OCP, and potential scan rate was 0.1 mV/s. Tafel polarization was carried out between -250 mV and +250 mV with respect to OCP, and the potential scan rate was 0.5 mV/s.

2.5 Measurement of the critical chloride concentration

At the onset of rebar corrosion, the specimen was splitted along the rebar by compression-testing machine and the corrosion on the surface can be observed; then one half of the specimen was cut off using a cutting machine to remove the boundary effect, only leaving the middle part of the concrete (ca. 150 mm long). Then this part of the concrete was placed in pulverizer, and powder samples were obtained layer by layer along the transport direction of chloride ions. The concentration of free chloride ions in the powder sample was measured using a chloride ion selective electrode. The concentration of chloride ions at a depth of 15 mm in the reinforcement cover is regarded as the critical chloride concentration.

3. RESULTS AND DISCUSSION

3.1 The analysis and criteria of the critical corrosion point of rebar

This work applies EIS method to monitor the corrosion of rebar in concrete, which includes qualitative and quantitative analysis. Qualitative analysis is usually applied on slight corrosion tendency, while quantitative analysis is used for noticeable corrosion tendency.

(1) Qualitative analysis of EIS

Cheng-hong Yang, Mei-lun Shi[9] gives a typical Nyquist graph about the passivated reinforcement in the reinforced concrete through analyzing the Nyquist graph theory, as shown in Figure 2. Can be seen from the figure in the Nyquist graph is made up of two time constant which shows a small semicircle and an oblique line (which is actually a small arc section of a big circle).When testing the actual reinforced concrete specimen , the frequency (ω) changing from high frequency to low frequency (ω ranged from ∞ to 0), and reflecting the response of the disturbance signal on the Nyquist graph which was caused by the respective parts of the reinforced concrete specimens, all the parts of the graphics stand for different kinetic parameters of the reinforced concrete system, including the high frequency part reflects the characteristics of the concrete and steel/concrete interface, and the low frequency part represents the characteristics of the passivation membrane on the surface of the steel. Therefore, can be respectively obtained the relevant information of the reinforced concrete and passivation membrane on the interface of steel/concrete by the curve change of high

frequency part or low frequency part. When Specific judgment Nyquist diagram can be observed in the low frequency curve, if it's a larger slope diagonals, denoting the passivation membrane on the surface of the steel in concrete is complete;If the slope of low frequency curve in figure is obviously reduced, the radius of the second semicircle present a limited number, the Nyquist shows distinctly two time constant, which explains the passivation membraneon the surface of the steel began to destroy.
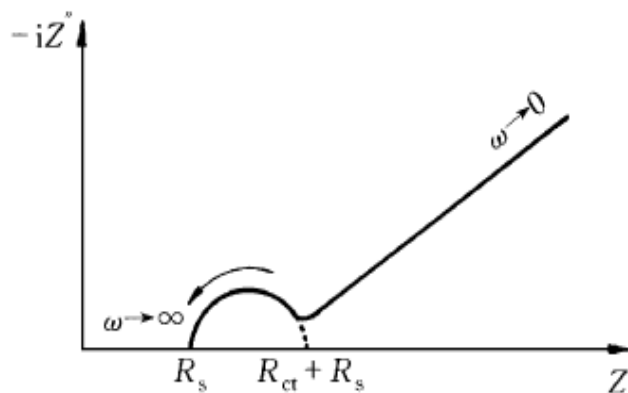
Figure 2. The typical Nyquist figure of reinforced concrete [9]

The electrochemical impedance spectra of the specimen in each group are shown in Fig.3 as a function of time (only one specimen is shown for each group). It can be seen that there are two capacitive loops in the Nyquist plots, corresponding to two time constants. In the beginning of the experiment, the capacitive loop in the low frequency region is a rising "straight line", which means the impedance and capacitance of the passive film are relatively large, and the rebar in the concrete is passive[10]. During the process of the experiment, the rising angle of the "straight line" decreases and becomes a small arc in the end. The change on the spectra indicates the onset of corrosion, i.e. the decrease of resistance and capacitance of the passive film. The qualitative analysis on the EIS can be used as a preliminary assessment on the corrosion of rebar, while more precise measurement (quantitative analysis) has been carried out on the impedance spectra using equivalent circuit.
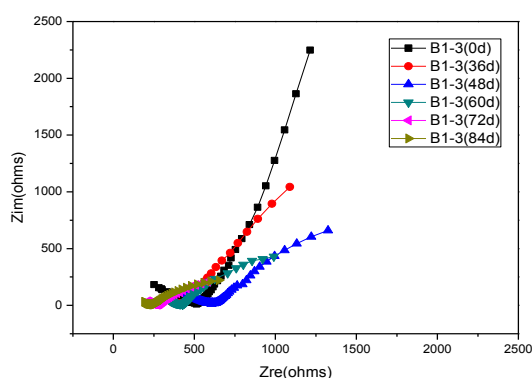
（a）EIS of specimen B1-3   （b）EIS of specimen A-1
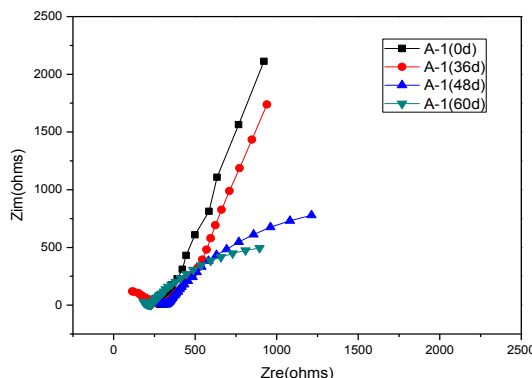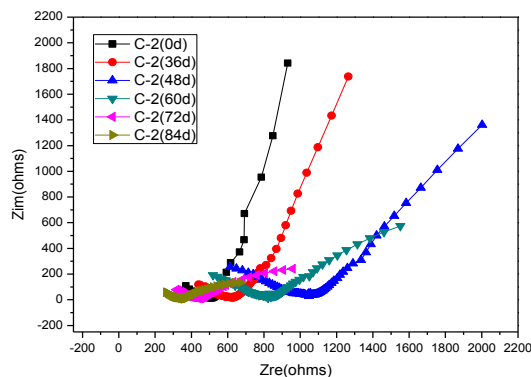
（c）EIS of specimen C-2
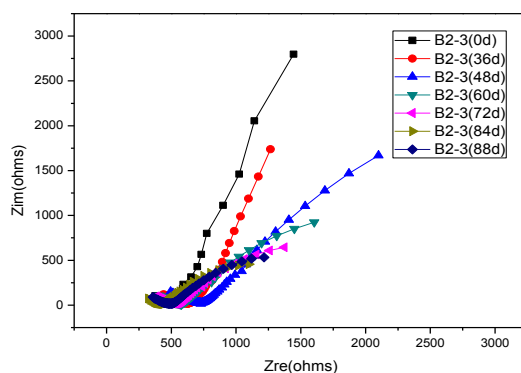
（d）EIS of specimen B2-3
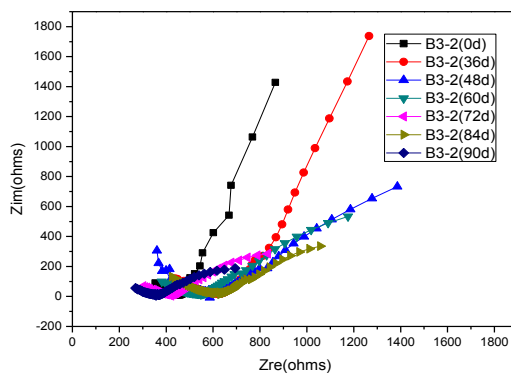
（e）EIS of specimen B3-2

Figure 3. EIS results with time

(2) Quantitative analysis of EIS

Quantitative analysis of EIS was immediately carried out when the qualitative analysis showed large corrosion tendency. Quantitative analysis started after 48d in the test. Firstly, ZSimpWin software should be used to fit the equivalent circuit (equivalent circuit was shown in Fig.4), obtaining the value of impedance and capacitance, analysing the passive film. Line polarization measurements and Tafel polarization measurements was used to manifest the corrosion of rebar at the onset of corrosion (which was shown in Fig.5). The results of quantitative analysis of the critical corrosion point of rebar are shown in Table 3, 4.
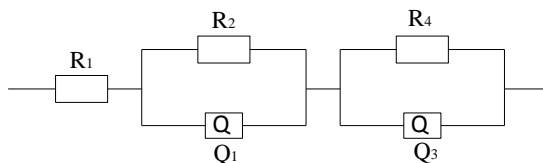
Note: R1 represents the resistance value of the solution; R2 represents the resistance value of concrete; R4 represents the electric double layer steel/concrete pore fluid interface electron transfer resistance

Figure 4. Equivalent circuit of corrosion of the rebar in concrete at the onset of corrosion

（a）LPR polarization curves   （b）Tafel polarization curves
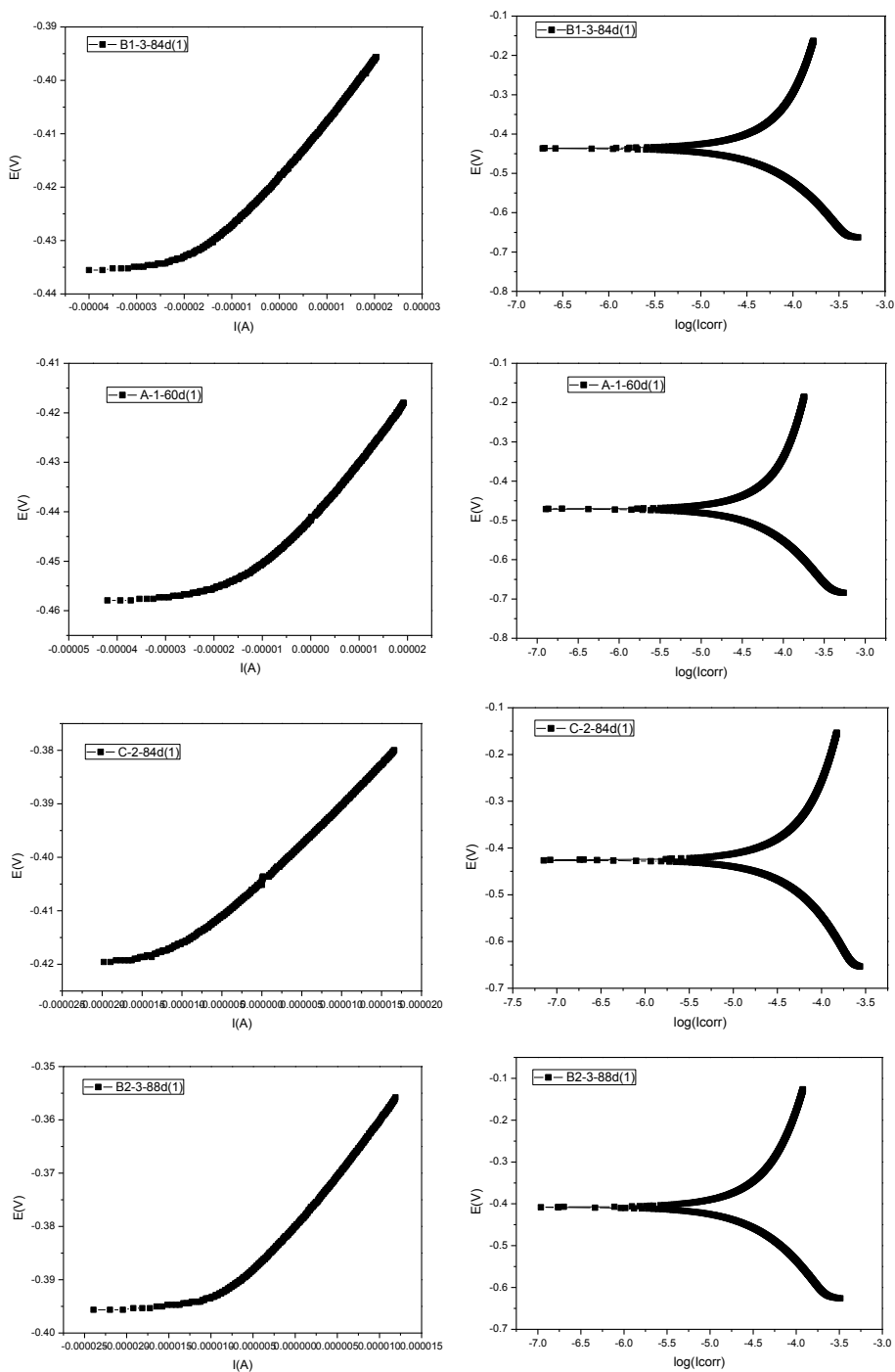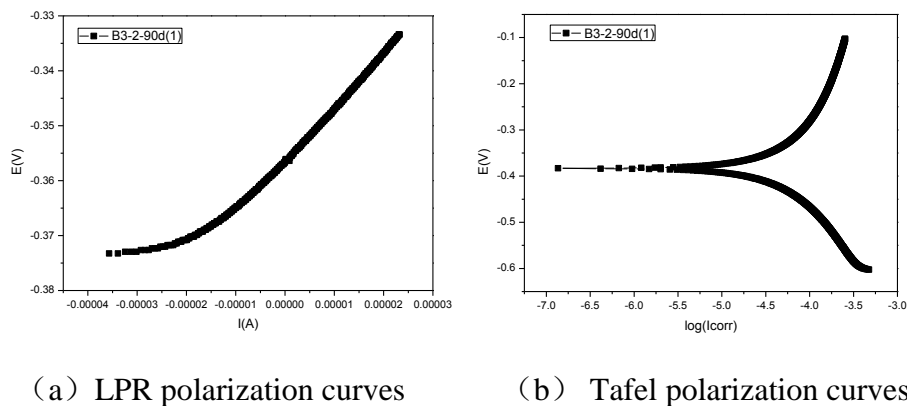
Figure 5. LPR and Tafel polarization curve of the specimens

Table 3. Data analysis of EIS equivalent circuit

specimen	R_1 (Ω/cm^2)	R_2 (Ω/cm^2)	R_4 (Ω/cm^2)	Chisq
B1-1-87	1.02E-07	1482	266.8	0.03299
B1-2-87	7.31E-11	1210	366.1	0.02308
B1-3-84	1.00E-07	787.4	254.6	0.02566
A-1-60	2.12E-06	597.2	229	0.01162
A -2-54	1.53E-08	345.3	195.8	0.03366
A -3-42	1.48E-05	558.1	218	0.01002
C-1-84	9.98E-06	1262	223.2	0.0287
C -2-84	1.00E-07	1220.8	264.1	0.0208
C -3-84	5.63E-05	392.9	320.6	0.004521
B2-1-88	2.04E-05	1378	296	0.01305
B2-2-88	0.0001962	1416	233.5	0.148
B2-3-88	7.49E-05	1552	318.4	0.02251
B3-1-90	2.90E-07	1910	274	0.0362
B3-2-90	1.00E-07	968.1	266.4	0.01261
B3-3-90	1.00E-07	313.6	292.4	0.02606

Note: number B1-1-87 represents the fitting data of No.1 in group B1 after 87d, and the value of Chisq represents degree of fitting, the lower it is the better the degree of fitting is.

Table 4. Data analysis of LPR and Tafel

specimen	LPR			Tafel	
	R_p (Ω/cm^2)	$E_{corr}(mV)$	$i_{corr}(\mu A/cm^2)$	E_{corr} (mV)	$i_{corr}(\mu A/cm^2)$
B1-1-87	1782.00	-388.36	12.20	-469.32	2.22
B1-2-87	1502.00	-391.79	14.47	-417.85	1.95
B1-3-84	1092.00	-418.38	19.90	-435.61	2.04
A-1-60	895.20	-402.66	11.13	-426.64	0.83
A-2-54	614.51	-408.68	35.38	-428.12	4.49
A-3-42	774.66	-406.40	28.06	-423.15	2.70

C-1-84	1441.00	-397.69	15.09	-416.47	3.48
C-2-84	1485.00	-405.00	14.63	-425.58	3.14
C-3-84	694.53	-446.66	31.30	-469.42	6.18
B2-1-88	1693.12	-387.12	21.89	-407.77	2.62
B2-2-88	1793.54	-440.66	24.33	-430.98	4.48
B2-3-88	1911.20	-380.59	10.69	-407.09	1.01
B3-1-90	2203.00	-403.88	35.03	-430.98	4.48
B3-2-90	1002.00	-356.94	21.68	-383.98	2.13
B3-3-90	494.68	-418.54	43.95	-442.47	5.61

Equivalent circuit fitting data from Nyquist graph could carry out a quantitative analysis about the degree of rebar corrosion in reinforced concrete, and meanwhile get some other parameters about the reinforced concrete specimen, which could more accurately estimate the degree of rebar corrosion in order to quantify the beginning of corrosion to get more accurate critical chloride ion density. Reference [9] came up with the typical reinforced concrete ac impedance spectra (Fig. 2) through theoretical analysis. The meanings of symbols in the Figure are as follows: (1) Rs is the limit value when ω→∞, on behalf of the resistance value of concrete pore solution, which is inversely proportional to the total porosity [11]; (2) Rct represent the diameter of the high frequency semicircle, on behalf of OH - reaction impedance in the pore solution. According to the parallel capillary bundle model of microstructure of concrete, the interior of the concrete is a network space composed by porosity and capillary. Due to the same reaction kinetics constants from the same block, Rct reflects that the contact reaction area of steel electrode and concrete surface is inversely proportional to the total surface area of all capillaries [12]; (3) C_{dl} can be obtained by the radius of the high frequency semicircle, represents the capacitance between electrodes and concrete surface, which is proportional to total surface area of all capillaries.

In addition, as shown in the comparison between table 3 and table 4, the fitting data is obtained from the data analysis of EIS and LPR. R4 that obtained from EIS shows that, due to the eliminated influence of Ohm drop, the transfer resistance of electric double layer from the interface area of reinforced concrete is a real polarization resistance. Moreover, the result of polarization Rp from LPR (linear polarization) actually includes two parts - R2 and R4, which could be proved by the result of (R2 + R4)/Rp close to 1 from the table. To sum up, R2 is the resistance value of concrete layer and R4 is the real polarization resistance value - Rp. Thus in fitting the equivalent circuit analysis (as shown in table 3), the resistance value of R4 (which is the polarization resistance Rp [13]) is basically all around 250 Ω/cm^2, according to the estimate criteria from Reference[10], steel passivation membrane has basically entered the stage of corrosion.

Then the linear polarization curve of the specimens and Tafel polarization curve (as shown in Figure 5 (a),(b) was fitting analysised, the fitting data as shown in table 4. The LPR fitting data can be found in the table, the Rp basically all around 1000Ω/cm^2 (note that this includes the resistance of concrete layer), corrosion potential Ecorr is about - 400 mv, corrosion current density icorr is about 20 mu A/cm^2; Furthermore, Tafel fitting data can be found in the table at the same time, the corrosion potential Ecorr is about - 400 mv, corrosion current density icorr approximately 3μA/cm^2. Furthermore, Table 4 indicates that the fitting data E_{corr} of LPR and Tafel test are close, while the i_{corr}

are of great difference, so we can know that the fitting data of LPR are just for the surface corrosion of the locate corroded points, it is just a locate value. While the fitting data of Tafel are for the surface corrosion of whole working electrode, so it is an average value. [14] Combined with the literature [10] [14] which give the judgment standards, through the comprehensive analysis including the ac impedance spectrum method, linear polarization method and Tafel polarization method, we can eventually determine the corrosion of rebar that reached a tipping point. In addition, the test that splitting the reinforced concrete test specimens can be found there are small amounts of corrosion products on the surface of rebar (at the stage of initial development of corrosion, as shown in Figure 7, more detailed analysis, please see section 3.2), and it's more advantageous to prove that the above-mentioned judgment is right.
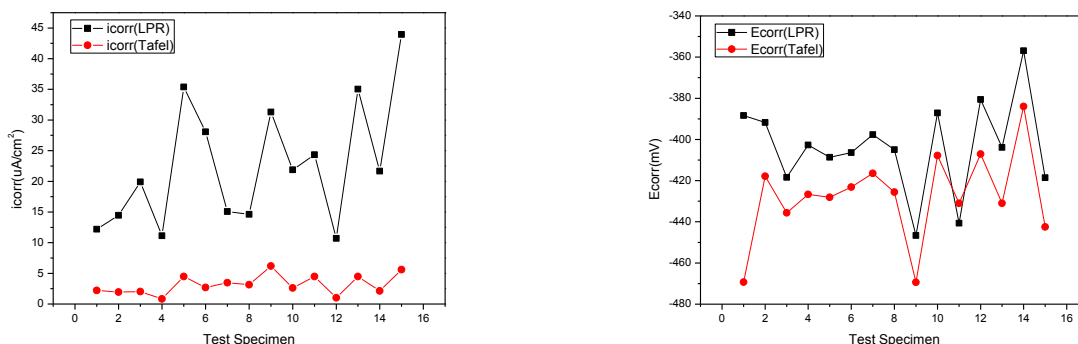
（a） The contrast analysis diagram about icorr   （b） The contrast analysis diagram about Ecorr

Figure 6. The contrast analysis diagram about icorr and Ecorr through the LPR and Tafel polarization method

In Table 3, the resistance values of R4 are about $250\Omega/cm^2$, and it shows that the film had been destroyed as reported in paper [10]. The resistance values of specimens B2-3-88 and C-3-84 range from 300 to $400\Omega/cm^2$, however, the LPR and Tafel test results in Table 4 and the observation by splitting the specimens show that the rebar enter the initial stage of corrosion, as shown in Fig.7. Compared with the standard in paper [10], middle or low corrosion rate can be obtained by the polarization resistance R_p, but high corrosion rate can be obtained by the corrosion current density i_{corr}, and medium high corrosion rate was observed by splitting the specimens. Thus errors exist in the corrosion tests of rebar, and the judgment of rebar corrosion should not limit to one method, but many methods should be combined for aggregate analysis. Based on the analysis of the test results, the $R_p=300\Omega/cm^2$ can be assumed to be the judgment standard of the corrosion critical point about reinforced in concrete.

Through the above test and the analysis, the critical corrosion point of rebar can be precisely manifested by qualitative and quantitative analysis of EIS, laying a good foundation of the study on critical chloride concentration.

（a）Rebar corrosion of B2-3　　　　　　　（b）Rebar corrosion of C-3
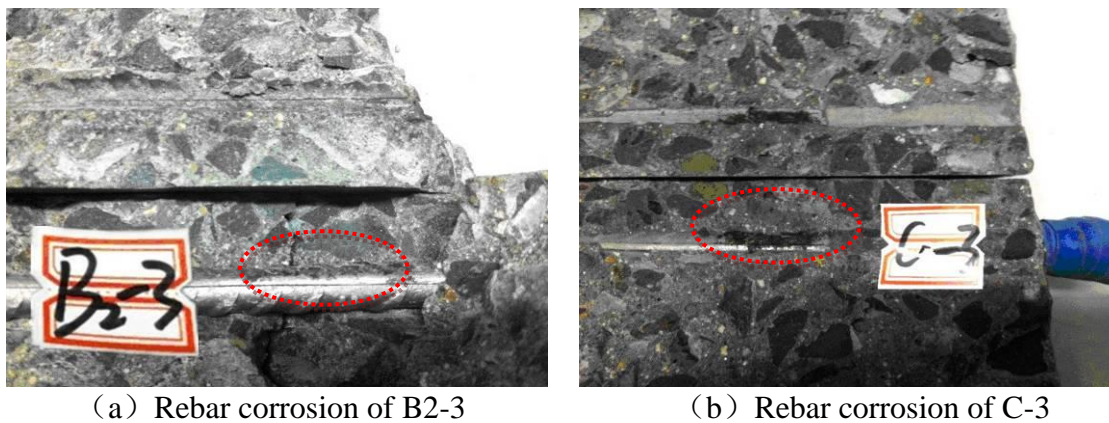
Figure 7. Rebar corrosion (observation by splitting)

3.2 SEM measurement

Scanning electron microscope (SEM) was used to observe the surface of the rebar samples which included corroded parts and the uncorroded parts. First of all, the uncorroded parts were observed, as shown in Fig.8. It can be seen that the surface of the rebar is rough, and there are a large number of cement hydration products (mainly needle stick ettringite) attached to the surface of rebar, but the distribution of crystallization is not uniform, and the passive film on the surface of rebar is also not uniform, however it is not destroyed.
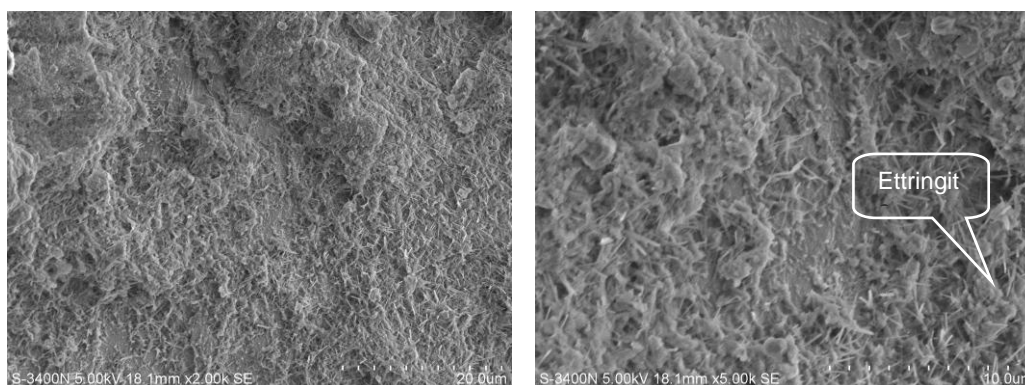
（a）Surface appearance of the uncorroded（b）Surface appearance of the uncorroded
　　　　　rebar(x2000)　　　　　　　　　　　　　　rebar(x5000)

Figure 8. SEM of surface appearance of the uncorroded rebar

Secondly, the corroded part of the rebar was observed, as shown in Fig.9. From Fig.9 (a), (b), it can be seen that the products of the corroded rebar are black, with dense structure (black rust Fe_3O_4), and some cracks existing on the surface of the corroded rebar. The reason may be that the chloride ions gathered on the surface of the rebar and entered through the weak part of the passive film, and reacted with the iron substrate. From Fig.9 (c), (d), we can see that there are evenly, loose corrosion products

(red rust $Fe_2O_3 \cdot xH_2O$) and obvious cracks on the surface of the rebar. It is mainly because the volume expansion of the red rust generated through the corrosion process resulted in corroded expansion cracks.
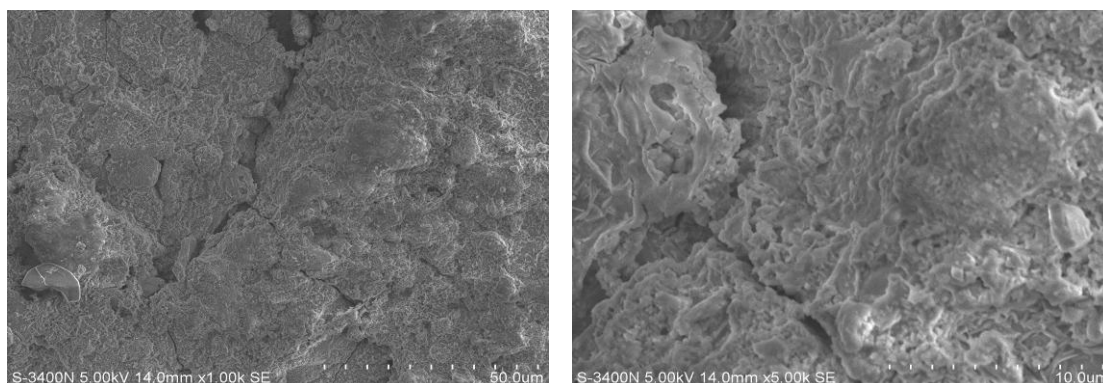
（a）Surface appearance of black rust (x1000)   （b）Surface appearance of black rust (x5000)
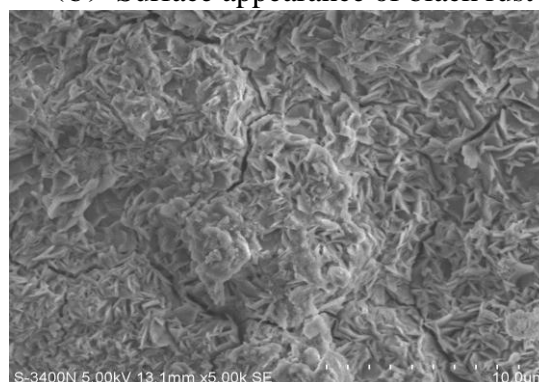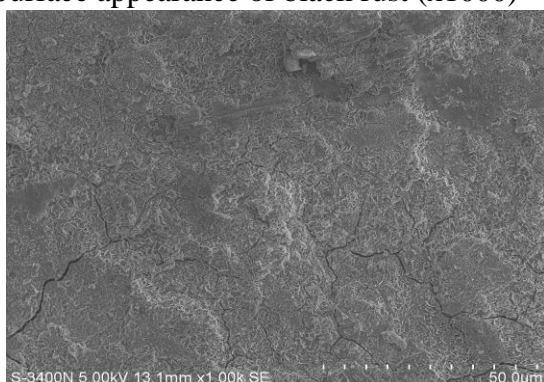
（c）Surface appearance of red rust (x1000)   （d）Surface appearance of red rust (x5000)

Figure 9. SEM of surface appearance of corroded rebar

Finally, the transition part of the corroded and uncorroded rebar surface was observed, as shown in Fig.10. It shows that the destroyed area of the passive film have some rust (mainly black rust Fe_3O_4, a small number of red rust $Fe_2O_3 \cdot xH_2O$). And the intact surface is still closely integrated with the cement hydration products, surface passive film is not destroyed. From the point of rebar corrosion situation, most of the rebar surface is black rust. The main reason is because, compared with Fe_2O_3, Fe_3O_4 has both trivalent iron ions and bivalent ferrous ions, so its corrosion products is not stable, but a product between passivation and corrosion. If O_2 and H_2O were cut off this moment, corrosion reaction will be terminated. Only in the case of O_2 diffusion enough, Fe_3O_4 can continue to generate stable oxide corrosion products Fe_2O_3. Through the above analysis, it shows that the rebar corrosion state was at the initial stage, as the onset of corrosion of rebar, and the concentration of chloride ions at the depth of reinforcement cover is regarded as the critical chloride concentration this moment.

（a）Surface appearance of the transition part(x2000)

（b）Surface appearance of the transition part(x5000)
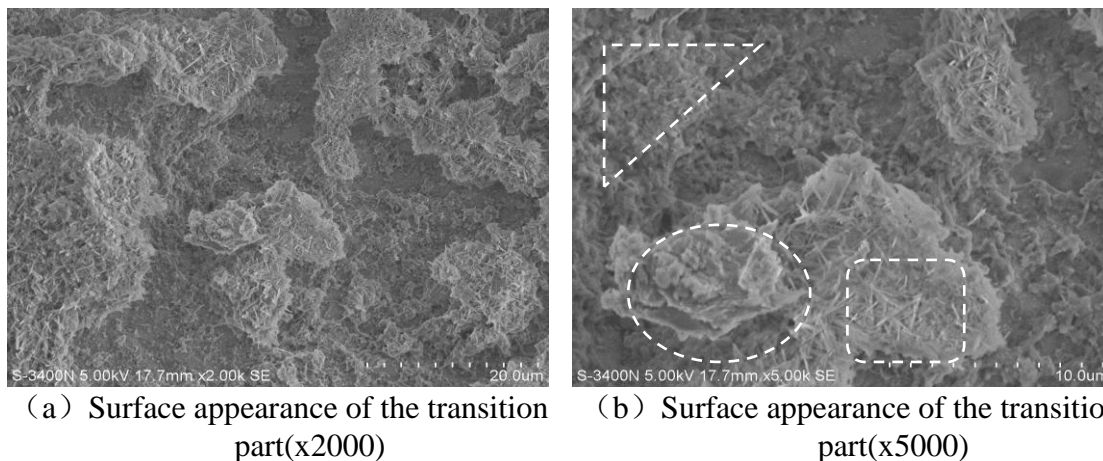
Note: In fig (6) oval area was red rust. Rectangle area was uncorroded part of the rebar passive film. Triangle area was black rust.

Figure 10. SEM of surface appearance of transition part of the corroded and uncorroded rebar surface

3.3 The impact analysis on ac impedance spectra of wet-dry cycling period

Ac impedance spectra of concrete specimens under different cycle are shown in Figure 11. It can be seen that obvious difference exists in the ac impedance spectra of the specimens under different cycle. With increasing period of wet-dry cycling, translation phenomenon of the spectra appeared on the complex plane. In addition, when the specimens are at the end of drying and soaking under the action of the different cycle, testing the saturation of them , as shown in Figure 12, we can see from the picture, in the case of dry-wet circulation time ratio remains the same (all are G: S = 3:1), with the increase of dry-wet cycle, the saturation of concrete block is similar at the end of soaking, but the saturation of them is decreased obviously at the end of drying. Through the above experiment can explain that the resistance and capacitance (indicators by the high frequency part) of concrete under different cycle produce differences due to the different degree of drying, namely, with increasing period of wet-dry cycling, the degree of drying for specimens increased, and the resistance of the concrete layer increased, which can be observed as translation of the spectra to the right on the complex plane.

（a）EIS after 0d

（b）EIS after 36d

（c）EIS after 48d　　　　　　（d）EIS after 60d

（e）EIS after 72d　　　　　　（f）EIS after 84d
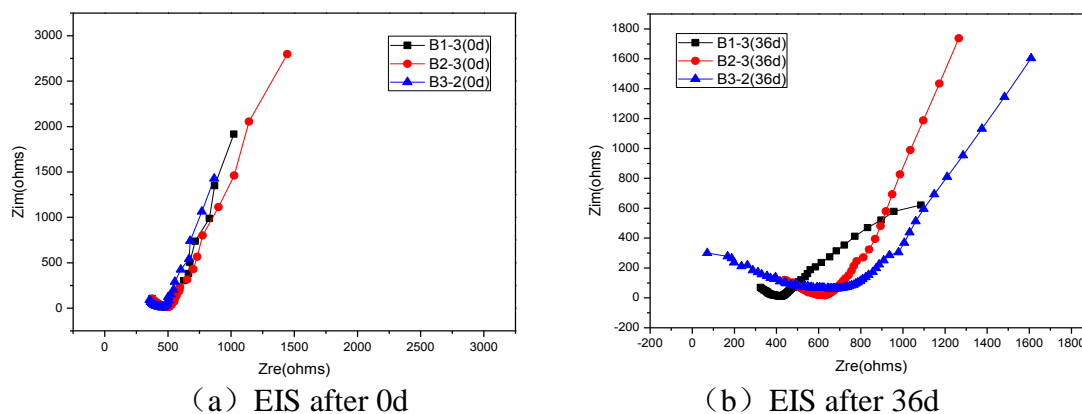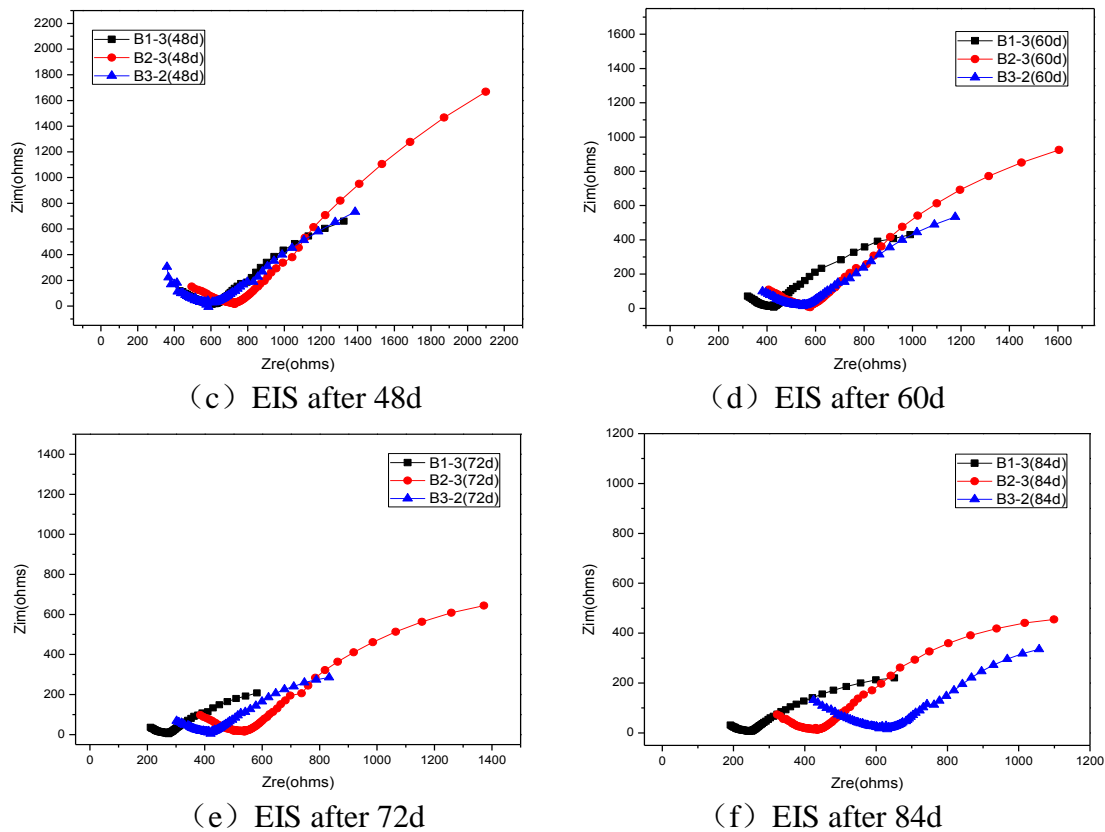
Figure 11. EIS of the specimens under different cycle
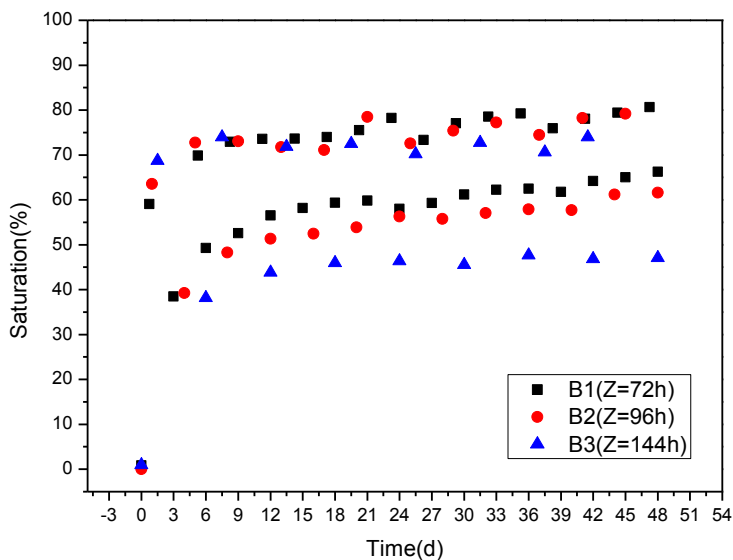
Figure 12. The change of saturation along with dry-wet cycles

In addition, it can be seen that although the spectra shows some translation, the rebar corrosion development process of B1, B2, B3 and other groups of specimens are almost the same (the topology of low frequency part changed almost the same), some exceptions of the specimens B1-3 existed after 36d, which may be caused by the test error.

3.4 The impact analysis on critical chloride ion concentration of wet-dry cycling period

When judging the rebar corrosion in concrete took place, its critical chloride concentration should be tested immediately according to the test process in section 2.5 of this paper. This sampling method is more reasonable than sampling by knocking mortar around reinforced to grind, because the chloride ions influencing rebar corrosion distribute in a small range around the rebar, it is difficult to control the sampling scope, causing test result greatly discrete. In addition, this method is compared with the embedded type chlorine ion selective electrode, although the method of embedded type chlorine ion selective electrode can get the targeted data on the point [15], its limitations is bigger, the influencing factors of test results is more, and it is also not convenient to apply it to the detection of practical engineering; while the method of filter pressing   can get more rational data, but this method can only get a regional average data, it turns out to be inaccurate in the case that chlorine ion is in gradient distribution[2]. Comprehensively comparative analysis, The sampling method of this article can avoid to produce larger human error, the result is more accurate and reliable.

The critical chloride concentration results of specimens under different wet-dry cycling are shown in Table 5. It can be seen that the critical chloride concentration increases slightly with increasing period of wet-dry cycling. The main reason is that with the increase of wet-dry cycling, the degree of drying for concrete increased, leading to the increasing of capillary absorption, which can absorb a lot of chloride ions in the process of immersing. But the diffusion of O_2 is restrained because of extending time of immersing, so rebar corrosion is delayed onset, and the critical chloride concentration increases.

Table 5. The critical chloride concentration under the action of different wet-dry cycling

Specimens	Cl^- （mol/L）	Percentage of concrete (%)	Percentage of binding material (%)	Average value of concrete (%)	Average value of binding material (%)
B1-1	0.004108	0.364	2.039		
B1-2	0.003326	0.295	1.651	0.318	1.780
B1-3	0.003326	0.295	1.651		
B2-1	0.004566	0.405	2.266		
B2-2	0.003829	0.339	1.900	0.357	2.000
B2-3	0.003697	0.328	1.835		
B3-1	0.000001	0.352	1.968		
B3-2	0.000001	0.339	1.900	0.347	1.946
B3-3	0.000001	0.352	1.968		

3.5 The impact analysis on EIS of fly ash content

EIS of concrete specimens under different content of fly ash are shown in Fig.13. It can be seen that, with the increase of fly ash content, obvious translation phenomenon of the spectra existed on the

complex plane. The main reason is that with the increase of fly ash content, the compactness of concrete increases, leading to the increase of the resistance and capacitance, which can be observed as translation of the spectra to the right on the complex plane (resistance increase), and the radius of capacitive loop increase obviously (capacitance increase), indicating that resistance R_s of concrete pore solution (that is, the equivalent circuit of the R2) increases with the increase of fly ash content. And it fits in with the literature [8] which described that the resistance R_s of concrete pore solution is inversely proportional to the total porosity.

（a）EIS after 0d （b）EIS after 36d

（c）EIS after 48d （d）EIS after 60d

（e）EIS after 72d （f）EIS after 84d
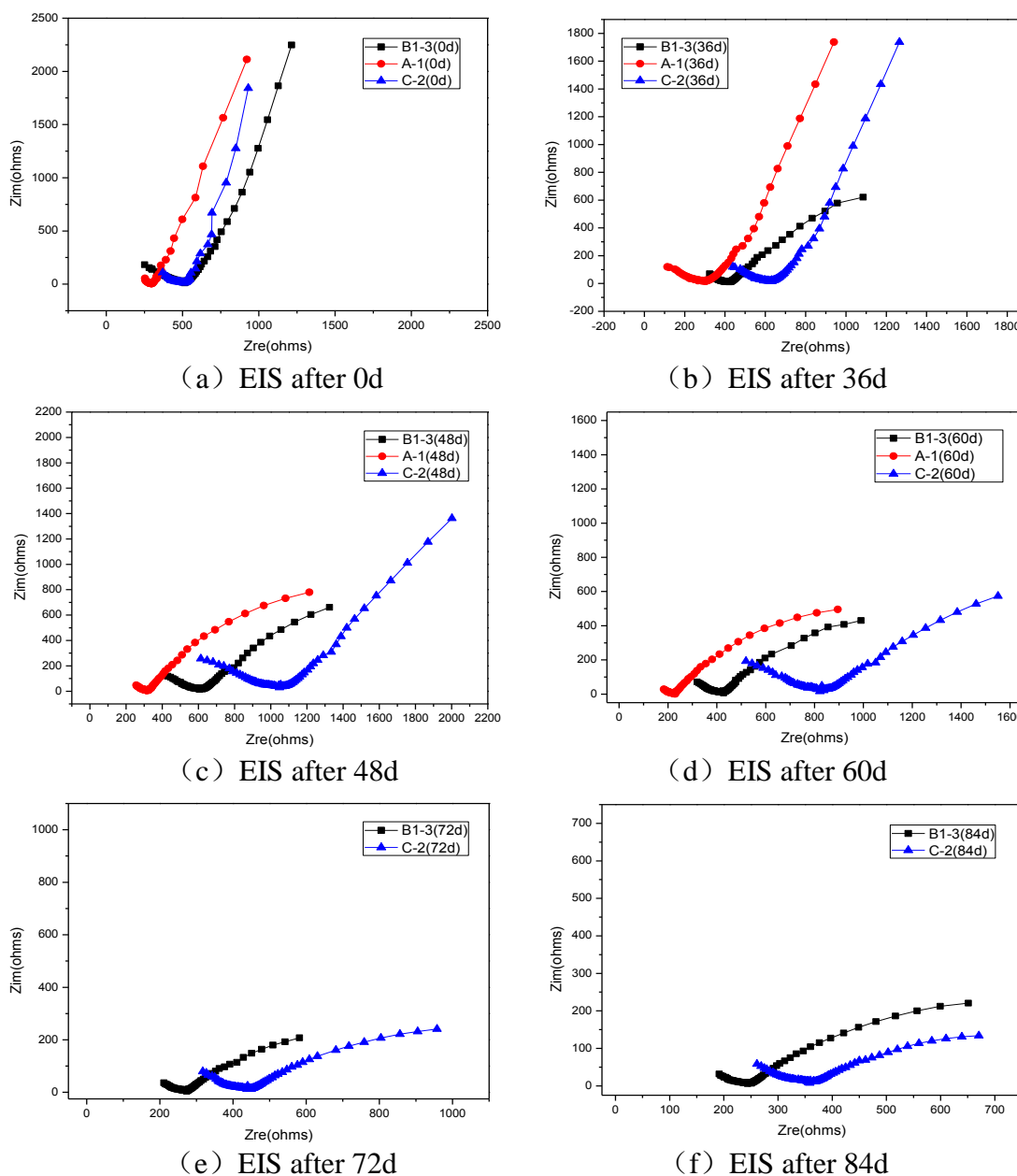
Note: The specimen A-1 rebar had been corroded since 72 days ago, so the EIS of specimen A-1 was not given in fig. (e), fig. (f)

Figure 13. EIS of the specimens under different dosage of fly ash

3.6 The impact analysis on the critical chloride ion concentration of fly ash content

When judging the rebar corrosion in concrete took place, the same method was used as before to test the critical chloride concentration of rebar corrosion, the results as shown in Table 6. It can be found that compared with group A, the critical chloride concentration of group B1 increase. It is mainly because the compactness of specimens of group B1 with 10% fly ash, leads to the reduce of the transmission speed of the Cl^-, O_2 and H_2O in the concrete, but pH value reduces a little, so the critical chloride concentration increases; And compared with group A, the compactness of group C increases, but the pH value of pore solution in concrete reduces because of the mix of fly ash, causing less chloride ion can break original chemical equilibrium, so the critical chloride concentration decreases.

Table 6. The critical chloride ion concentration under different fly ash content

Specimens	Cl^-（mol/L）	Percentage of concrete (%)	Percentage of binding material (%)	Average value of concrete (%)	Average value of binding material (%)
A-1	0.004108	0.364	2.039		
A-2	0.003569	0.316	1.771	0.298	1.671
A-3	0.002423	0.215	1.203		
B1-1	0.004108	0.364	2.039		
B1-2	0.003326	0.295	1.651	0.318	1.780
B1-3	0.003326	0.295	1.651		
C-1	0.003445	0.305	1.710		
C-2	0.003211	0.285	1.594	0.282	1.579
C-3	0.002889	0.256	1.434		

4. CONCLUSIONS

Ac impedance method can precisely manifest the critical corrosion point of rebar, the $Rp=300\Omega/cm^2$ can be assumed to be the judgment standard of the corrosion critical point about reinforced in concrete. The critical chloride concentration of concrete specimens increase with increasing period of wet-dry cycling approximately. Small content of fly ash can increase the critical chloride concentration of rebar corrosion in concrete, but when adding the content of fly ash, even if the compactness of concrete is improved, the critical chloride concentration in concrete pore solution will also reduce with the reduce of the pH value. With increasing period of wet-dry cycling, the degree of drying of the specimens increases, and the resistance of the concrete layer increases, characterizing the translation of spectra to the right on the complex plane; With the increase of fly ash content, the compactness, the resistance and the capacitance of concrete increase, characterizing the translation of the spectra to the right on the complex plane.

References

1. H. Böhni, *Corrosion in Reinforced Concrete Structures*, Wood head Publishing Limited, Cambridge(2005)
2. U. Angst, B. Elsener, C. K. Larsen, Ø. Vennesland, *Cem. Concr. Res.*, 39(2009)1122-1138.
3. K. Ann and H. Song, *Corros. Sci.*, 49(2007) 4113-4133
4. M. Kouřil, P. Novák and M. Bojko, *Cem. Concr. Res.*, 40(2010)431-436
5. J.X. Xu, L.H. Jiang, W.L. Wang and Y. Jiang, *Constr. Build. Mater.*, 25(2011)663-669
6. J.X. Xu, L.H. Jiang and J.X. Wang, *Constr. Build. Mater.*, 23(2009)1902-1908
7. U.M. Angst, A. Rønnquist, B. Elsener, C. K. Larsen and Ø. Vennesland, *Corros. Sci.*, 53(2011)177-187
8. Y. Li.*Nanjing:Nanjing water conservancy scientific research institution*,(2003).
9. Zh.H. Yang, M.L. Shi, *J. Build. Mater.*, 2 (1999) 81-84.
10. S. G. Millard, D. Law, J. H. Bungey, *NDT &E Int.*, 34(2001)409-417.
11. D.H. Hong, *Beijing: China Railway Publishing House*, 1998.
12. M.L. Shi, Zh.Y. Chen, *J. Chin. Ceram. Soc.*, 25(1997) 241.
13. Ch. Xu , Zh.Y. Li and W.L. Jin, *Corro. Sci. Prot. Tech.*, 5 (2011)393-398.
14. X.L. Zhang, Zh.H. Jiang, Zh.P. Yao, Y. Song and Zh.D. Wu, *Corros. Sci.*,51(2009)581-587.
15. U. M. Angst, B. Elsener, C. K. Larsen, Ø. Vennesland, *Corros. Sci.*, 53(2011)1451-1464.